Chapter 3

Advanced Receivers for MIMO HSDPA

Martin Wrulich, Christian Mehlführer,
and Markus Rupp

Contents

3.1 Overview

The performance of Wideband Code Division Multiple Access (WCDMA) networks is limited due to interference more than by any other single effect. Frequency-selective channels cause a loss of orthogonality between the utilized spreading codes and impose restrictive throughput constraints.

Modern receiver design has to face these difficulties and tries to circumvent them without increasing the complexity to unacceptable levels.

This chapter covers the development of a multi-user, intra-cell, interference-aware minimum mean squared error (MMSE) equalizer for the transmit antenna array (TxAA) mode of multiple-input, multiple-output (MIMO) High-Speed Downlink Packet Access (HSDPA). The resulting receiver is able to exploit the special structure imposed by the precoded TxAA transmission to efficiently suppress the interference by only moderately increasing the complexity (compared to the classical single-user (SU) equalizer). The solution can be interpreted as a multi-user extension of the classical MMSE equalizer for HSDPA systems.

In this chapter we define a suitable system model to derive the intra-cell interference-aware MMSE equalizer and investigate its capabilities to suppress the multi-user intra-cell interference for TxAA HSDPA-operated networks. The resulting throughput performance is then investigated by means of physical layer as well as system-level simulations.

3.2 Introduction

HSDPA has been standardized as an extension of the Universal Mobile Telecommunications System (UMTS) as a part of the 3rd Generation Partnership Project (3GPP) Release 5 [1]. It is spectrally the most efficient WCDMA system commercially available at the moment. To satisfy the need for higher data rates and new services with the current base station sites, even higher cell capacities and spectral efficiencies must be achieved. Correspondingly, 3GPP has considered numerous proposals that incorporate MIMO techniques for the enhancement of frequency division duplex (FDD) HSDPA [2]. 3GPP has chosen the dual-stream transmit antenna array (D-TxAA) as the MIMO scheme for FDD because of its backward compatibility with TxAA [3]. In D-TxAA, a second data stream is transmitted via spatial multiplexing when user equipment with two receive antennas experiences high channel quality. If channel quality is low, the transmission mode is switched to TxAA, which is also the supported mode when the user equipment has only one receive antenna available. In contrast to D-TxAA, TxAA allows for scheduling multiple users simultaneously, exploiting multi-user diversity.

The intra-cell interference caused by the loss of orthogonality between the spreading codes due to the frequency-selective channel imposes restrictive throughput constraints. To combat this effect in HSDPA MMSE equalizers are disposed [4–7]. However, these solutions do not take multi-user operation or the interference structure in the cell into account.

A second approach to combat interference is the so-called interference mitigation that can be performed at the transmitter and/or the receiver

side. In particular, in the downlink, each receiver needs to detect a *single* desired signal, while experiencing two types of interference. These are caused by the serving Node-B (intra-cell interference) and by a few dominant neighboring Node-Bs (inter-cell interference). Handling the interference on the receiver side is a difficult job, especially in the multi-user case in which classical approaches result in complex receiver structures [8–10]. To ease the job of the receiver, the precoding has been optimized for specific receiver structures; see, for example, [6,7,11]. Because HSDPA implicitly utilizes multi-code operation in the downlink, care also must be taken to design the receiver appropriately [12]. For D-TxAA, the multiple stream operation can be further utilized by successive interference cancellation (SIC) receivers [13]. More practical investigations on this subject were also conducted by 3GPP [14], but so far none of these recommendations have been implemented. Given the limited battery capabilities of today's handsets, complexity is an important issue. Despite the available research, the combined effects in the case of the precoded multi-user multi-code operation have not been addressed thus far.

In the uplink, on the other hand, the base station receiver has to detect *all* desired users in the cell, while also suppressing neighboring cell interference from many different sources [15]. A good overview about the interference situations in the uplink and downlink case, together with some well-known solutions for them, can be found in [16].

When interference mitigation is performed at the transmitter, accurate channel state information from all users is needed [17]. This requires lots of signaling and feedback information exchange, which typically is not available in cellular contexts.

A novel approach to cope with the problems of TxAA HSDPA is an interference-aware MMSE equalizer that utilizes the spatial structure of the intra-cell interference, that is, the precoding state of the cell. In particular, the receiver introduced in this chapter is able to effectively suppress the multi-user interference with moderate complexity. Further details on the explanations here can also be found in [18–20].

3.3 Transmit Antenna Array (TxAA) Mode

TxAA was introduced with UMTS in 1999 and now builds the foundation of the spatial multiplexing enhancement in MIMO HSDPA [3]. In contrast to the double-stream operation of MIMO HSDPA, TxAA allows for multiple users being served in the downlink simultaneously, which is called *multi-code scheduling*. Multi-code scheduling is well suited to work optimally in terms of the sum-rate throughput and short-term fairness trade-off [21]. Future-generation mobile networks implicitly build on similar concepts;

for example, Long-Term Evolution (LTE) [22] puts a strong emphasis on multi-user scheduling in its time-frequency downlink frames.

In TxAA HSDPA, every user is assigned a specific number of orthogonal spreading sequences of length 16. At a maximum, 15 spreading sequences can be assigned to all users, the 16th orthogonal spreading sequence is reserved for transmitting the pilot channels and other control channels. Depending on the link-adaptation feedback in the form of channel quality indicator (CQI) values, the scheduler can decide which users should be served in parallel. Furthermore, note that the TxAA scheme allows for an arbitrary number of receive antennas being utilized at the user equipment (UE).

3.3.1 System Model

Figure 3.1 shows the TxAA transmission scheme for one receive antenna when U users are simultaneously served. We define the spread and scrambled chip stream of user u at time instant i as

$$\mathbf{s}_i^{(u)} \triangleq \left[s_i^{(u)}, \ldots, s_{i-L_b-L_f+2}^{(u)} \right]^T \tag{3.1}$$

where L_b and L_f are the length of the channel impulse response and the equalizer length, respectively. Thus, the vector $\mathbf{s}_i^{(u)}$ contains the $L_b + L_f - 1$ recent chips. We assume that the power σ_s^2 of the chip stream $\mathbf{s}_i^{(u)}$ of each user u is normalized to one.

By multiplying $\mathbf{s}_i^{(u)}$ by a factor $\alpha^{(u)}$, the base-station can allocate a certain amount of transmit power to each served user. After the power

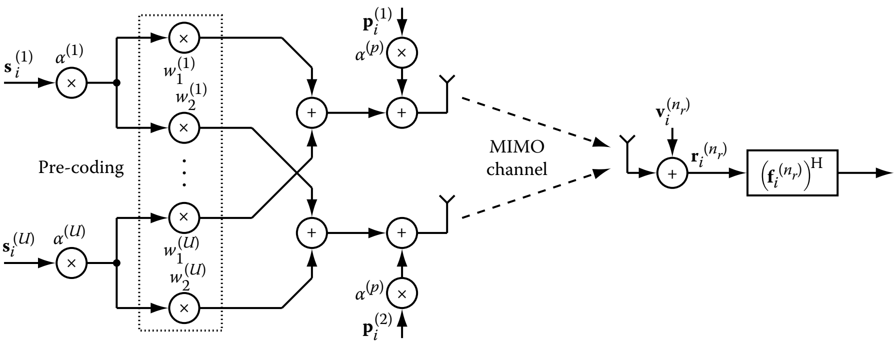

Figure 3.1 Multi-user transmission in TxAA for a total number U of simultaneously served users. The precoding is conducted individually for every user. At the receiver, only one receive antenna is depicted, although the scheme allows for an arbitrary number of receive antennas.

allocation, the chip streams are weighted by the user-dependent complex precoding coefficients $w_1^{(u)}$ and $w_2^{(u)}$ at the first and second transmit antennas, respectively. Our modeling holds for arbitrary precoding weights, but we want to note that due to standardization, these coefficients are strongly quantized [2], which we will take advantage of later. The weighted chip streams of all users are then added to the sequences $\alpha^{(p)}\mathbf{p}_i^{(1)}$ and $\alpha^{(p)}\mathbf{p}_i^{(2)}$, representing the sum of all channels that are transmitted without precoding, that is, the Common Pilot CHannel (CPICH), the High-Speed Shared Control CHannel (HS-SCCH), and other signaling channels—to which we will refer as non-data channels.

The frequency-selective channel between the n_tth transmit and the n_rth receive antennas is represented in Figure 3.2 by the vector $\mathbf{h}^{(n_r,n_t)}$, $n_t = 1, 2 = N_T$, $n_r = 1, \ldots, N_R$, composed of the taps of the channel. If we neglect for the moment the non-data channels, $\alpha^{(p)}\mathbf{p}_i^{(1)}$ and $\alpha^{(p)}\mathbf{p}_i^{(2)}$, the multi-user transmission in Figure 3.1 can be represented by U virtual antennas, one for each active user, as illustrated in Figure 3.2. The resulting equivalent (virtual) channels between user u and receive antenna n_r are then given by $\tilde{\mathbf{h}}^{(u,n_r)} = w_1^{(u)}\mathbf{h}^{(n_r,1)} + w_2^{(u)}\mathbf{h}^{(n_r,2)}$, $u = 1, 2, \ldots, U$. From this description it can be seen immediately that the intra-cell interference observed by user u can be treated as being transmitted over U different channels. The classical MMSE equalizer, however, would be determined only by the precoding weights $w_1^{(u)}$ and $w_2^{(u)}$ and would not consider the special structure of the interference. Thus, the degraded transmission scheme of TxAA imposes an interference situation that cannot be handled well by the classical MMSE equalizer, which is matched only to the channel of the desired user. This is in contrast to the single-input, single-output (SISO) HSDPA case, where due to the lack of precoding, the interference of simultaneously served users is transmitted over the same channel as the one of the desired user. Thus, in SISO HSDPA, equalization of the desired user's signal also equalizes the signal of the simultaneously served users.

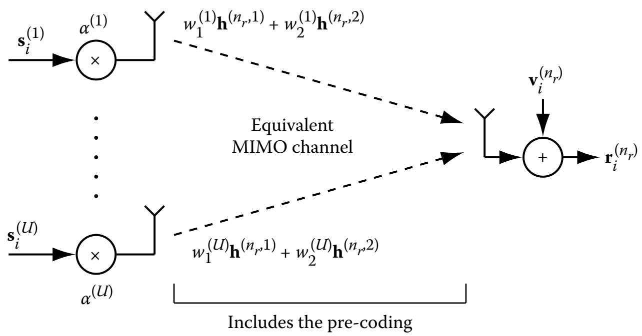

Figure 3.2 Equivalent representation of the multi-user TxAA transmission, representing U virtual antennas and U virtual channels.

For the derivation of our intra-cell interference-aware MMSE equalizer, let us define the $L_f \times (L_h + L_f - 1)$-dimensional band matrix modeling the channel between the n_tth transmit and the n_rth receive antenna:

$$\mathbf{H}^{(n_r,n_t)} = \begin{bmatrix} h_0^{(n_r,n_t)} & \cdots & h_{L_h-1}^{(n_r,n_t)} & & 0 \\ & \ddots & & \ddots & \\ 0 & & h_0^{(n_r,n_t)} & \cdots & h_{L_h-1}^{(n_r,n_t)} \end{bmatrix}, \quad n_t = 1, 2, \quad n_r = 1, \ldots, N_R \tag{3.2}$$

The full frequency-selective MIMO channel can be modeled by a block matrix $\mathbf{H}$ consisting of $N_R \times 2$ band matrices:

$$\mathbf{H} = \begin{bmatrix} \mathbf{H}^{(1,1)} & \mathbf{H}^{(1,2)} \\ \vdots & \vdots \\ \mathbf{H}^{(N_R,1)} & \mathbf{H}^{(N_R,2)} \end{bmatrix} \tag{3.3}$$

where we explicitly put in the assumption that for TxAA, only two transmit antennas ($N_T = 2$) are utilized.

By stacking the received signal vectors of all N_R receive antennas,

$$\mathbf{r}_i = \left[\left(\mathbf{r}_i^{(1)}\right)^{\mathrm{T}}, \cdots, \left(\mathbf{r}_i^{(N_R)}\right)^{\mathrm{T}} \right]^{\mathrm{T}} \tag{3.4}$$

and by stacking the transmitted signal vectors of all U users and the vectors $\mathbf{p}_i^{(1)}$ and $\mathbf{p}_i^{(2)}$,

$$\mathbf{s}_i = \left[\left(\mathbf{s}_i^{(1)}\right)^{\mathrm{T}}, \cdots, \left(\mathbf{s}_i^{(U)}\right)^{\mathrm{T}}, \left(\mathbf{p}_i^{(1)}\right)^{\mathrm{T}}, \left(\mathbf{p}_i^{(2)}\right)^{\mathrm{T}} \right]^{\mathrm{T}} \tag{3.5}$$

we obtain the compact system description:

$$\mathbf{r}_i = \underbrace{\mathbf{H}(\mathbf{W} \otimes \mathbf{I}_{L_h+L_f-1})}_{\mathbf{H}_w} \mathbf{s}_i + \mathbf{v}_i = \mathbf{H}_w \mathbf{s}_i + \mathbf{v}_i \tag{3.6}$$

Here, $\otimes$ denotes the Kronecker product, and $\mathbf{v}_i$ is an additive noise vector that can incorporate both the thermal noise and the interference from other base-stations (inter-cell interference). The $2 \times (U+2)$ dimensional matrix $\mathbf{W}$ contains the precoding coefficients $w_1^{(u)}$ and $w_2^{(u)}$ of all users, as well as their power coefficients $\alpha^{(u)}$ ($u = 1, 2, \ldots, U$) and the power coefficients $\alpha^{(p)}$,

and is defined as

$$\mathbf{W}^{(\mathrm{MU})} \triangleq \begin{bmatrix} \alpha^{(1)} w_1^{(1)} \cdots \alpha^{(U)} w_1^{(U)} & \alpha^{(p)} & 0 \\ \alpha^{(1)} w_2^{(1)} \cdots \alpha^{(U)} w_2^{(U)} & 0 & \alpha^{(p)} \end{bmatrix} \tag{3.7}$$

This matrix reflects the premise that the non-data channels are not precoded; thus the two columns on the right side are specified solely by the single parameter $\alpha^{(p)}$, which controls the total power spent on these channels. In general, we also assume that the power available at the base station is fully spent; thus the coefficients α are prone to a sum-power constraint:

$$\sum_{u=1}^{U} \left(\alpha^{(u)}\right)^2 + 2\left(\alpha^{(p)}\right)^2 = P \tag{3.8}$$

3.4 Interference-Aware MMSE Equalization

Having our system model being specified as in the previous section, we are now able to derive the resulting MMSE equalizer. Without loss of generality, we assume in the following that the sequence of User 1 is to be reconstructed. The MMSE equalizer coefficients can be calculated by minimizing the quadratic cost function [23]:

$$J(\mathbf{f}) = \mathbb{E}\left\{\left|\mathbf{f}^{\mathrm{H}}\mathbf{r}_i - s_{i-\tau}^{(1)}\right|^2\right\} \tag{3.9}$$

with τ specifying the delay of the equalized signal, fulfilling $\tau \geq L_h$ due to causality. In this work, we assume the channel to be known at the receiver site.

This cost function minimizes the distance between the equalized chip stream and the transmitted chip stream. In Equation (3.9), the vector $\mathbf{f}$ defines N_R equalization filters:

$$\mathbf{f} = \left[\left(\mathbf{f}^{(1)}\right)^{\mathrm{T}}, \cdots, \left(\mathbf{f}^{(N_R)}\right)^{\mathrm{T}}\right]^{\mathrm{T}} \tag{3.10}$$

Each filter $\mathbf{f}^{(n_r)} = [f_0^{(n_r)}, \ldots, f_{L_f-1}^{(n_r)}]^{\mathrm{T}}$ has a length L_f. Note that because of the definition of $\mathbf{f}$ and $\mathbf{r}_i$, the inner product $\mathbf{f}^{\mathrm{H}}\mathbf{r}_i$ can be implemented by summing the outputs of the N_R equalization filters $(\mathbf{f}^{(n_r)})^{\mathrm{H}}$. This sum then yields the MMSE estimate of the transmitted chip sequence.

The minimization of the cost function can be performed by deriving Equation (3.9) with respect to $\mathbf{f}^*$ [24], evaluating the expectation operation,

and setting the derivative equal to zero:

$$\frac{\partial J}{\partial \mathbf{f}^*} = \left(\mathbf{H}_w \mathbf{R}_{ss} \mathbf{H}_w^{\mathrm{H}} + \mathbf{R}_{vv}\right) \mathbf{f} - \sigma_s^2 \mathbf{H}_w \mathbf{e}_\tau = 0 \tag{3.11}$$

The matrices $\mathbf{R}_{ss}$ and $\mathbf{R}_{vv}$ are the signal and noise covariance matrices, respectively, and the vector $\mathbf{e}_\tau$ is a zero vector of length $(U+2)(L_h+L_f-1)$ with a single "1" at cursor position τ. The equalizer coefficients for the data stream of the first user are therefore given by

$$\mathbf{f} = \sigma_s^2 \left(\mathbf{H}_w \mathbf{R}_{ss} \mathbf{H}_w^{\mathrm{H}} + \mathbf{R}_{vv}\right)^{-1} \mathbf{H}_w \mathbf{e}_\tau \tag{3.12}$$

If the transmitted data signals of the users are uncorrelated with equal power σ_s^2, the covariance matrix $\mathbf{R}_{ss}$ becomes $\sigma_s^2\mathbf{I}$, and if we assume the noise vector $\mathbf{v}_i$ white with variance σ_v^2, the noise covariance matrix becomes $\sigma_v^2\mathbf{I}$. Without losing generality, we can assume that the signal covariance σ_s^2 is equal to 1 because the individual transmit powers of the users are determined by $\alpha^{(u)}$. The variance σ_v^2 is composed of the thermal noise and the power received from the other base stations. Note that if the receiver takes the structure of the inter-cell interference into account, effort must be expended to obtain an accurate estimation of the covariance matrix $\mathbf{R}_{vv}$.

Because this equalizer considers the interference of all users in the cell due to the full knowledge of the matrix $\mathbf{W}^{(\mathrm{MU})}$, we call it an intra-cell interference-aware MMSE equalizer. The standard equalizer is a special case of our solution and neglects the interference from other users, which we consequently call single-user (SU) equalizer in the following. It can be calculated from Equation (3.12) using the single-user precoding weight matrix of rank 1

$$\mathbf{W}^{(\mathrm{SU})} = \begin{bmatrix} \alpha^{(1)} w_1^{(1)} \\ \alpha^{(1)} w_2^{(1)} \end{bmatrix} \mathbf{e}_1^{\mathrm{T}} \tag{3.13}$$

instead of the multi-user precoding weight matrix $\mathbf{W}^{(\mathrm{MU})}$. Here, $\mathbf{e}_1$ is a zero column-vector of length $U+2$ and a "1" at the first position. If only a single user is receiving data in the cell, both equalizers are very similar, with the only difference being that the intra-cell interference-aware equalizer also considers the interference generated by the non-data channels.

3.4.1 Interference Suppression

Before assessing the throughput performance of our proposed MMSE equalizer, we first want to look at the interference suppression capabilities. To do so, we adapted the model in [25], which describes the post equalization and despreading signal-to-interference-plus-noise ratio (SINR) for

arbitrary linear receivers in a multi-stream closed-loop MIMO Code Division Multiple Access (CDMA) system. The remaining intra-cell interference after equalization—for a specific channel realization and precoding state—generated by the desired user and all other active users is explicitly given by

$$P_{\text{intra}} = \sum_{\substack{m=0 \\ m \neq \tau}}^{L_b+L_f-2} \left|\mathbf{f}^{\mathrm{H}} \boldsymbol{\gamma}_m^{(1)}\right|^2 + \sum_{u=2}^{U} \sum_{\substack{m=0 \\ m \neq \tau}}^{L_b+L_f-2} \left|\mathbf{f}^{\mathrm{H}} \boldsymbol{\gamma}_m^{(u)}\right|^2 \tag{3.14}$$

with $\boldsymbol{\gamma}_m^{(u)}$ denoting the mth column of the user-dedicated channel matrix

$$\mathbf{H}^{(u)} = \mathbf{H}\left(\left[\alpha^{(u)} w_1^{(u)}, \alpha^{(u)} w_2^{(u)}\right]^{\mathrm{T}} \otimes \mathbf{I}_{L_b+L_f-1}\right) \tag{3.15}$$

Because Equation (3.14) depends on the current realization of the precoding state, we cannot use it directly to evaluate the performance of our proposed equalizer for general conditions. Thus, we approximate the remaining intra-cell interference by its expectation over the precoding state of the interfering users. Given a certain number of active users in the cell, the remaining intra-cell interference after equalization then becomes

$$\mathbb{E}_w\{P_{\text{intra}}\} = \underbrace{\sum_{\substack{m=0 \\ m \neq \tau}}^{L_b+L_f-2} \left|\mathbf{f}^{\mathrm{H}} \boldsymbol{\gamma}_m^{(1)}\right|^2}_{f_{\text{self}}} + \sum_{u=2}^{U} \underbrace{\mathbb{E}_w\left\{\sum_{\substack{m=0 \\ m \neq \tau}}^{L_b+L_f-2} \left|\mathbf{f}^{\mathrm{H}} \boldsymbol{\gamma}_m^{(u)}\right|^2\right\}}_{f_{\text{other}}} \tag{3.16}$$

with f_{self} and f_{other} denoting the determinative factors for the self and other-user intra-cell interference remaining after equalization, and $\mathbb{E}_w\{\cdot\}$ being the expectation with respect to the precoding coefficients w_1, w_2 of the interfering users.

As already mentioned, the 3GPP specifies a quantized codebook of possible precoding vectors [2]. The UE is responsible for evaluating and signaling the precoding vector that leads to the best pre-equalization SINR. It is important to note that the CQI feedback must be evaluated jointly with the precoding to obtain good throughput results [26]. Given the precoding codebook of [2], in [27] we are also able to show that in D-TxAA—even if multi-code scheduling would be implemented—an equalizer has no possibility to exploit information about the precoding state of the cell to suppress intra-cell interference.

Table 3.1 lists the simulation parameters we applied to evaluate the capability of our proposed equalizer to suppress the intra-cell interference caused by the other active users in the cell. Figures 3.3 and 3.4 show the performance in terms of the interference suppression capabilities, both for the self interference f_{self} and the other-user interference f_{other}, assuming

Table 3.1 Simulation Parameters for Figures 3.3 and 3.4

Parameter	*Value*
Simulated slots	1000
Slot time	2/3 ms
Receive antennas N_R	2
Precoding codebook	3GPP TxAA [2]
Equalizer span L_f	40 chips
Equalizer delay τ	20 chips
Precoding delay	11 slots
Mobile speed	3 km/h
Channel profile	ITU Pedestrian B (PedB) [28]
Active users U	4
Fading model	Improved Zheng model [29,30]

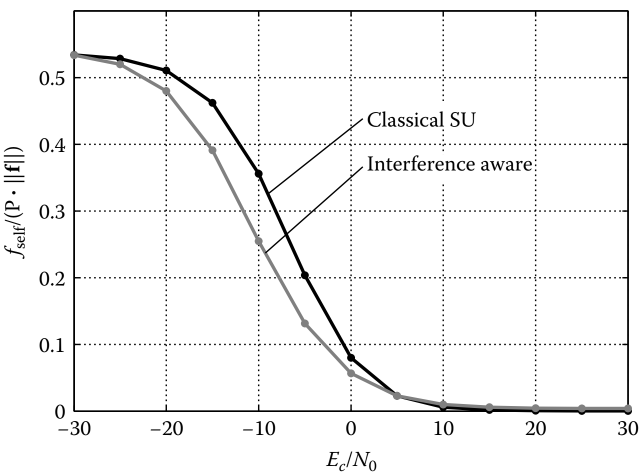

Figure 3.3 Self intra-cell interference f_{self} performance comparison of the proposed intra-cell interference aware equalizer and the classical single-user equalizer, assuming perfect knowledge of the cell's precoding state.

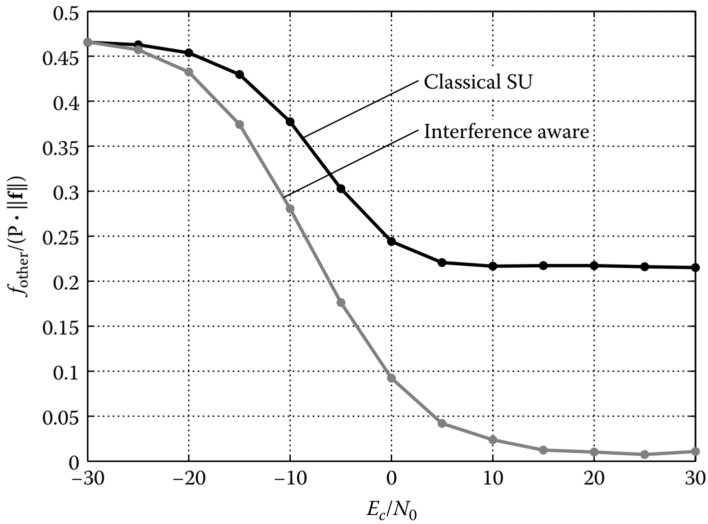

Figure 3.4 Other-user intra-cell f_{other} performance comparison of the proposed intra-cell interference-aware equalizer and the classical single-user equalizer, assuming perfect knowledge of the cell's precoding state.

perfect knowledge of the cell's precoding state. We normalize the two coefficients by the total received interference power (that is, because the channel is by assumption already normalized to 1) by dividing by the norm of the equalizer $\|\mathbf{f}\|$ and the total transmitted intracell power P, defined in Equation (3.8). It can be observed that our proposed equalizer is able to outperform the classical single-user equalizer, especially in terms of the other-user intra-cell interference when the chip-level signal-to-noise ratio (SNR) E_c/N_0 becomes high. The classical single-user equalizer is not able to cancel the interference generated by the transmission to other users, leading to a saturation of f_{other}. In contrast, our proposed equalizer can effectively decrease this interference term. The self intra-cell interference suppression is similar for higher E_c/N_0 values because the single-user equalizer is also matched to the channel of the desired user, which is sufficient to be able to restore the spreading code orthogonality, that is, lower f_{self}.

3.4.2 Complexity

Given the solution to the interference-aware MMSE equalization in Equation (3.12), it is interesting to assess the additional complexity needed to compute our proposed filter. Assuming uncorrelated transmit sequences with constant power, that is, $\mathbf{R}_{ss} = \sigma_s^2\mathbf{I}$, the additional complexity can be

evaluated by looking at the product $\mathbf{H}_w \mathbf{R}_{ss} \mathbf{H}_w^{\mathrm{H}} \propto \mathbf{H}_w \mathbf{H}_w^{\mathrm{H}}$ that is needed in the inverse part of $\mathbf{f}$. By writing

$$\mathbf{H}_w \mathbf{H}_w^{\mathrm{H}} = \mathbf{H}\left(\mathbf{W}^{(\mathrm{MU})}\left(\mathbf{W}^{(\mathrm{MU})}\right)^{\mathrm{H}} \otimes \mathbf{I}_{L_b+L_f-1}\right)\mathbf{H}^{\mathrm{H}} \tag{3.17}$$

it can easily be seen that the additional cost of our proposed equalizer is determined only by the larger matrix multiplication of $\mathbf{W}^{(\mathrm{MU})}(\mathbf{W}^{(\mathrm{MU})})^{\mathrm{H}}$ instead of $\mathbf{W}^{(\mathrm{SU})}(\mathbf{W}^{(\mathrm{SU})})^{\mathrm{H}}$, which is low compared to the cost of, for example, the inverse.

In particular, if we assume the complexity of matrix multiplications to be of order $\mathcal{O}\{K^3\}$ (with K being the larger matrix dimension), the added complexity of considering the multi-user precoding matrix is of order $\mathcal{O}\{(U+2)^3\}$. The matrix inverse, however, is of order $\mathcal{O}\{(N_R L_f)^3\}$, and because U is typically much smaller than L_f in practical systems, the multiplication of the muli-user precoding matrix is negligible.

3.5 Precoding State

In TxAA HSDPA, the MIMO channel is estimated by utilizing the CPICH, similar to UMTS. To be able to calculate the receive filter for the data channel, that is, the High-Speed Downlink Shared CHannel (HS-DSCH), however, the mobile needs to know (1) the *power offset* of the individual High-Speed Physical Downlink Shared CHannel (HS-PDSCH) compared to the CPICH, and (2) the *precoding coefficients* that the base station applied for the transmission. The power offset is signaled by higher layers [31], and the precoding coefficients of all simultaneous transmissions are signaled on the according HS-SCCH [32,33], where every active user has its own channel. This unfortunately makes things difficult for our proposed equalizer because the HS-SCCHs are scrambled with user-specific scrambling sequences[1], thus making it impossible to monitor the precoding state of the other users.

To overcome this problem, three different solutions are possible:

1. Change the signaling scheme in the HS-SCCH such that all active users know about the whole precoding state in the cell.
2. Include some training data in the HS-PDSCHs of the users to estimate the precoding state.
3. Blindly estimate the precoding state.

[1] The scrambling sequence in HSDPA is a function of the user identification number, known only to the base station and the particular user.

From this list, the first solution would require a change in the transmission standard [34], and thus is unfeasible for a practical implementation. Also the second solution, the training data-based approach, is not directly portable and would require network equipment vendors to implement algorithms of additional complexity in the base station, as well as the reservation of spreading code resources. The blind estimation solution seems thus far the most practicable approach that does not require any changes in the current standard and does not reduce the available resources in the CDMA cell.

Blind estimation is generally quite a challenging task, in particular in a multi-user context. Typical approaches treat the unknown inputs—in this case the unknown transmit data **s**—as *nuisance parameters* that the estimator must cope with in order to supply blind estimates of the parameters of interest. The Maximum Likelihood (ML) principle provides a systematic way to deduce the Minimum Variance Unbiased (MVU) estimator, maximizing the joint likelihood function [35]. There exist a number of possibilities to avoid the joint estimation of all parameters, that is, the power coefficients $\alpha^{(u)}$ and the data **s**. The *unconditional* or stochastic ML criterion models the vector of nuisance parameters as a random vector and maximizes the marginal of the likelihood function conditioned to **s**. Unfortunately, the unconditional ML estimator is generally unknown because the expectation with respect to **s** cannot be solved in closed form. However, in the low SNR regime, the unconditional likelihood function becomes quadratic in the observation with independence of the statistical distribution of the nuisance parameters. Nevertheless, this estimator class is generally difficult to solve and works only reasonably well in the low SNR regime [35].

Another modern approach for this kind of problems is based on random set theory [9], which can be utilized to find optimum estimators for random vectors when both the length and the values of the vector components are unknown. In the context of the precoding state estimation, the random vector to be estimated would be the vector of power coefficients $\alpha^{(u)}$, $u = 1, \ldots, U$, and $\alpha^{(p)}$, where the values of the coefficients as well as the length of the vector are unknown, because U is unknown. Applying random set theory leads to optimum Bayesian ML estimators. However, these require a joint estimation of the data sequence and the precoding state, which is typically computationally very demanding and thus disadvantageous for battery-powered mobile devices.

In [20] we propose a second-order Gaussian ML estimator that is able to estimate the precoding state of the cell with reasonable complexity. Due to the difficulty of the estimation problem, the estimator performance is far from optimum, but is sufficient to allow the multiuser interference-aware MMSE equalizer to closely achieve the performance when the precoding state is perfectly known. As the treatment of the precoding state estimation

would go beyond the scope of this chapter, we refer the reader to [20] for further details.

3.6 Performance Evaluation

We split our performance evaluation into two different parts: (1) physical-layer simulations for a fixed transmission setup of TxAA HSDPA and (2) system-level simulations with adaptive feedback and scheduling. Each simulation approach has a different focus, with the physical-layer simulations covering channel encoding and decoding, W-CDMA processing, as well as the receiver processing in detail. On the other hand, system-level simulations represent a whole HSDPA network with adaptive feedback, scheduling, and Radio Resource Control (RRC) algorithms.

3.6.1 Physical-Layer Simulation Results

We conducted physical-layer simulations utilizing a standard compliant HSDPA simulator. The simulation assumptions in Table 3.2 correspond

Table 3.2 Simulation Parameters for Physical-Layer Simulations

Parameter	*Value*
Active users U	4
Desired user CQI	13
Interfering HS-PDSCH E_c/I_{or}	[−6, −8, −10] dB
Interfering user CQIs	{16, 11, 8}
Interfering user precoding	$\left\{\begin{bmatrix}1\\ \frac{1}{\sqrt{2}}(+1-j)\end{bmatrix}, \begin{bmatrix}1\\ \frac{1}{\sqrt{2}}(-1+j)\end{bmatrix}, \begin{bmatrix}1\\ \frac{1}{\sqrt{2}}(-1-j)\end{bmatrix}\right\}$
Precoding codebook	3GPP TxAA [2]
CPICH E_c/I_{or}	−10 dB
Other non-data channel E_c/I_{or}	−12 dB
UE capability class	6
Channel profile	ITU Pedestrian A (PedA), , Pedestrian B (PedB)
UE speed	3 km/h

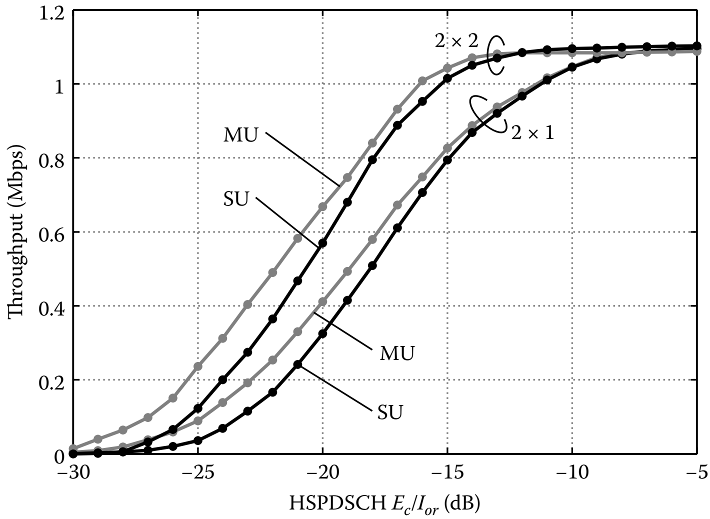

Figure 3.5 Throughput of desired user in a spatially uncorrelated ITU PedA channel at CQI 13, corresponding to a maximum throughput of 1.14 Mbps.

to a cell in which four users are receiving data simultaneously. User 1 is moving through the cell and obtains the precoding coefficients as adaptively requested, according to the definition in the standard [2]. The three interfering users are assumed to be stationary; thus, their precoding coefficients and transmit power do not change. In these simulations we assume that all users are always scheduled with the same CQI value, that is, no link adaptation other than the precoding is performed.

The achieved data throughput of User 1 in PedA and PedB environment is plotted in Figure 3.5 and Figure 3.6, respectively. In both scenarios, the interference-aware equalizer with perfect knowledge of the precoding state significantly outperforms the single-user equalizer. In the figures, E_c/I_{or} denotes the ratio of the average transmit energy per chip (E_c) to the total transmit power spectral density (I_{or}) [32].

The gain in the PedB channel in Figure 3.6 is much larger than the gain in the PedA channel, which has a much shorter maximum delay spread. This is caused by the larger loss of orthogonality in the PedB environment and the subsequently larger post equalization interference.

For a larger number of receive antennas, the simulation results show larger performance gains. The interference-aware equalizer can effectively utilize the spatial information to suppress the interfering signals. The largest performance increase of the interference-aware equalizer was found for the 2×2 PedB environment with 4 dB.

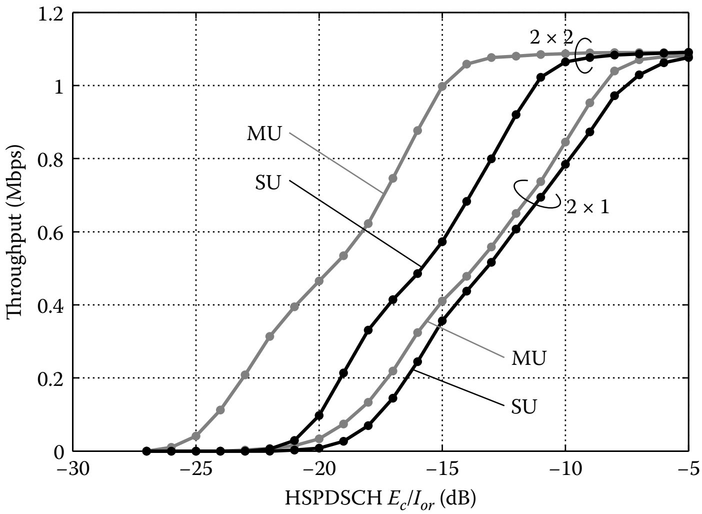

Figure 3.6 Throughput of desired user in a spatially uncorrelated ITU PedB channel at CQI 13, corresponding to a maximum throughput of 1.14 Mbps.

3.6.2 System-Level Results

To assess performance on the network level, we also conducted a set of system-level simulations with the simulator described in [25,27]. The simulation assumptions in Table 3.3 correspond to a 19-site scenario with a homogenous network load in which the multi-code scheduler serves four active users simultaneously. All 25 simulated users are moving through the cell with random directions and are adaptively reporting their CQI and precoding feedback according to their capability class [3]. The feedback delay was set to 11 slots.

The distributions of the SINR for the PedA and PedB channels, averaged over all active users in the cell, are plotted in Figure 3.7. It can be observed that the interference-aware (multi-user (MU)) equalizer is able to deliver significantly higher SINRs for PedB channels. In the PedA environment, the gain is negligible.

Figure 3.8 shows the average sector throughput. The interference-aware (MU) equalizer outperforms the classical (SU) equalizer significantly, again with more remarkable gains in the PedB environment—up to 11.7%.

Table 3.3 Simulation Parameters for System-Level Simulations

Parameter	*Value*
Simultaneously active users U	4
Transmitter frequency	1.9 GHz
Base station distance	1000 m
Total power available at Node-B	20 W
CPICH power	0.8 W
Power of other non-data channels	1.2 W
Spreading codes available for HSDPA	15
Macro-scale pathloss model	Urban micro [36]
Scheduler	Round Robin
Stream power loading	Uniform
Users in the cell	25
Cell deployment	Layout type 1 [37]
Precoding codebook	3GPP TxAA [2]
UE capability class	10
Equalizer span	40 chips
Feedback delay	11 slots
Channel profile	ITU Pedestrian A (PedA), Pedestrian B (PedB)
UE speed	3 km/h, random direction
Simulation time	25,000 slots, each 2/3 ms

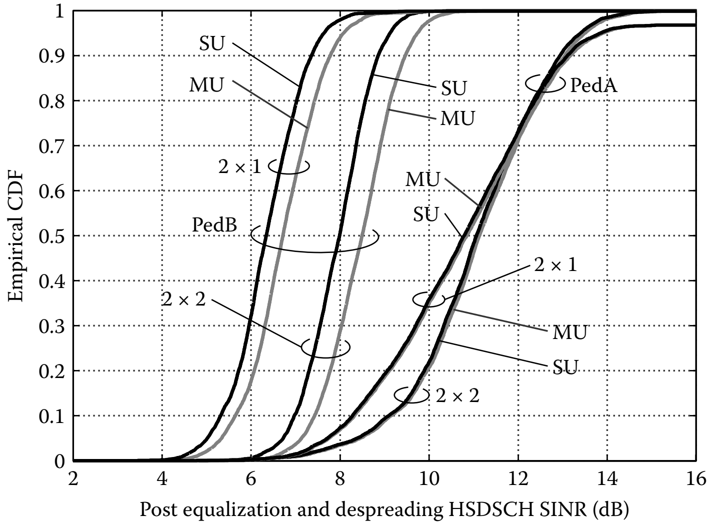

Figure 3.7 Empirical CDFs of the post equalization and despreading SINR of the HS-DSCH.

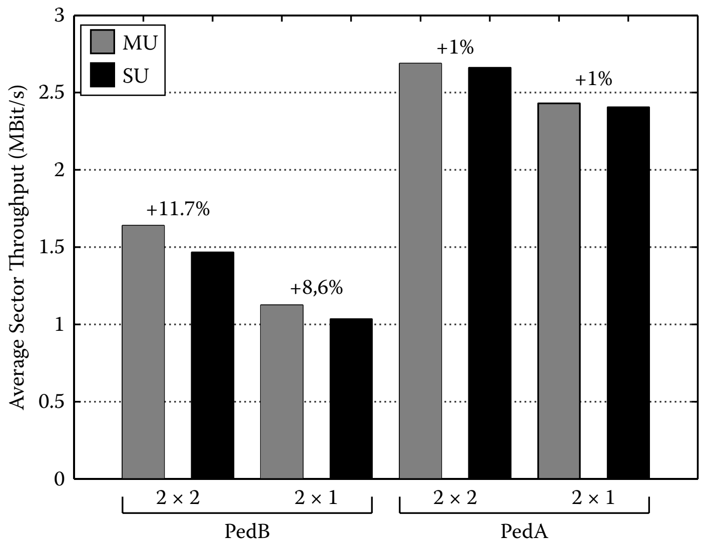

Figure 3.8 Average sector throughput results in the network specified by Table 3.3.

3.7 Summary

This chapter introduced a system model for TxAA HSDPA that takes the structure of the intra-cell interference in case of multi-code scheduling into account. The consideration of all simultaneously served users in the derivation of the MMSE equalizer leads to an interference-aware equalizer that has only slightly increased complexity compared to the classical SU MMSE equalizer. Simulations showed greatly reduced post equalization interference for the interference-aware equalizer. Finally, this chapter presented the performance gain of the introduced equalizer by means of physical-layer and system-level simulations. The results showed that the performance gains of the interference-aware MMSE equalizer increase with the frequency selectivity or, equivalently, the delay spread of the channel and the number of receive antennas. Both simulation types identified the new receiver structure as superior to the classical approach.

Acknowledgments

This work was funded by mobilkom austria AG and the Christian Doppler Laboratory for Wireless Technologies for sustainable Mobility. The views expressed are those of the authors and do not necessarily reflect the views within mobilkom austria AG.

References

[1] H. Holma and A. Toskala, *WCDMA for UMTS—Radio Access for Third Generation Mobile Communications*, 3rd ed., John Wiley & Sons, 2005.

[2] Technical Specification Group Radio Access Network, Multiple-Input Multiple-Output UTRA, 3rd Generation Partnership Project (3GPP), Tech. Rep. TR 25.876 Version 7.0.0, March 2007.

[3] Technical Specifiation Group Radio Access Network, Physical Layer Procedures (FDD), 3rd Generation Partnership Project (3GPP), Tech. Rep. TS 25.214 Version 7.4.0, March 2007.

[4] L. Mailaender, Linear MIMO equalization for CDMA downlink signals with code reuse, *IEEE Trans. Wireless Commun*., 4(5): 2423–2434, September 2005.

[5] M. Melvasalo, P. Janis, and V. Koivunen, MMSE equalizer and chip level inter-antenna interference canceler for HSDPA MIMO systems, in *Proc. IEEE 63rd Vehicular Technology Conf. Spring (VTC)*, 4: 2008–2012, 2006.

[6] S. Shenoy, M. Ghauri, and D. Slock, Receiver designs for MIMO HSDPA, in *Proc. IEEE Int. Conf. Commun. (ICC)*, 2008, pp. 941–945.

[7] H. Zhang, M. Ivrlac, J.A. Nossek, and D. Yuan, Equalization of multiuser MIMO high speed downlink packet access, in *Proc. IEEE 19th Int. Symp. Personal, Indoor and Mobile Radio Commun. (PIMRC)*, 2008, pp. 1–5.

[8] F. Petre, M. Engels, A. Bourdoux, B. Gyselinckx, M. Moonen, and H.D. Man, Extended MMSE receiver for multiuser interference rejection in multipath DS-CDMA channels, in *Proc. IEEE VTS 50th Vehicular Technol. Conf. Fall (VTC)*, 3: 1840–1844, 1999.

[9] E. Biglieri and M. Lops, Miltiuser detection in a dynamic environment. I. User identification and data detection, *IEEE Trans. Inf. Theory*, 53(9): 3158–3170, September 2007.

[10] E. Virtej, M. Lampinen, and V. Kaasila, Performance of an intra- and inter-cell interference mitigation algorithm in HSDPA system, in *Proc. IEEE 67th Vehicular Technology Conference Spring (VTC)*, 2008, pp. 2041–2045.

[11] S. Shenoy, I. Ghauri, and D. Slock, Optimal precoding and MMSE receiver designs for MIMO WCDMA, in *Proc. IEEE 67th Vehicular Technology Conference Spring (VTC)*, 2008, pp. 893–897.

[12] B.-H. Kim, X. Zhang, and M. Flury, Linear MMSE space-time equalizer for MIMO multicode CDMA systems, *IEEE Trans. Commun*., 54(10): 1710–1714, 2006.

[13] D. Bosanska, C. Mehlführer, and M. Rupp, Performance evaluation of intra-cell interference cancelation in D-TxAA HSDPA, in *Proc. ITG International Workshop on Smart Antennas (WSA)*, Darmstadt, Germany, February 2008, pp. 338–342.

[14] Technical Specification Group Radio Access Network, Feasibility Study on Interference Cancellation for UTRA FDD User Equipment (UE), 3rd Generation Partnership Project (3GPP), Tech. Rep. TR 25.963 Version 7.0.0, April 2007.

[15] A. Nordio and G. Taricco, Linerar receiver interfaces for multiuser MIMO communications, in *Proc. Eur. Signal Processing Conf. (EUSIPCO)*, 2006.

[16] J. Andrews, Interference cancellation for cellular systems: A contemporary overview, *IEEE Wireless Commun. Mag*., 12(2): 19–29, April 2005.

[17] H. Zhang and H. Dai, Cochannel interference mitigation and cooperative processing in downlink multicell multiuser mimo networks, *EURASIP J. Wireless Commun. Netw*., 2: 222–235, December 2004.

[18] M. Wrulich, C. Mehlführer, and M. Rupp, Interference aware MMSE equalization for MIMO TxAA, in *Proc. IEEE 3rd Int. Symp. Commun. Control and Signal Processing (ISCCSP)*, 2008, pp. 1585–1589.

[19] C. Mehlführer, M. Wrulich, and M. Rupp, Intra-cell interference aware equalization for TxAA HSDPA, in *Proc. IEEE 3rd Int. Symp. Wireless Pervasive Computing*, 2008, pp. 406–409.

[20] M. Wrulich, C. Mehlführer, and M. Rupp, Managing the interference structure of MIMO HSDPA: A multi-user interference aware MMSE receiver with moderate complexity, *IEEE Transactions on Wireless Communications*, Vol. 9, No. 3, Mar. 2010.

[21] D.I. Kim and S. Fraser, Two-best user scheduling for high-speed downlink multicode CDMA with code constraint, in *Proc. IEEE Global Telecommun. Conf. (GLOBECOM)*, 4: 2569–2663, 2004.

[22] Technical Specification Group Radio Access Network, Evolved Universal Terrestrial Radio Access (E-UTRA); LTE Physical Layer—General Description, 3rd Generation Partnership Project (3GPP), Tech. Rep. TS 36.201 Version 8.3.0, March 2009.

[23] J. Proakis, *Digital Communications*, 4th ed., McGraw-Hill Science Engineering, August 2000.

[24] S. Haykin, *Adaptive Filter Theory*, 4th ed., Prentice-Hall, 2002, ISBN 978-0-13-090126-2.

[25] M. Wrulich, S. Eder, I. Viering, and M. Rupp, Efficient link-to-system level model for MIMO HSDPA, in *Proc. IEEE 4th Broadband Wireless Access Workshop*, 2008.

[26] C. Mehlführer, S. Caban, M. Wrulich, and M. Rupp, Joint throughput optimized CQI and precoding weight calculation for MIMO HSDPA, in *Proc. 42nd Asilomar Conf. Signals, Systems and Computers*, October 2008.

[27] M. Wrulich and M. Rupp, Computationally efficient MIMO HSDPA system-level evaluation, *EURASIP Journal on Wireless Communications and Networking*, vol. 2003, Article ID382501, 14 pages, 2009. doi: 10.1155/2009/382501.

[28] Members of ITU, Recommendation ITU-R M.1225: Guidelines for Evaluation of Radio Transmission Technologies for IMT-2000, International Telecommunication Union (ITU), Tech. Rep., 1997.

[29] Y. Zheng and C. Xiao, Simulation models with correct statistical properties for rayleigh fading channels, *IEEE Trans. Commun*., 51(6): 920–928, June 2003.

[30] T. Zemen and C. Mecklenbräuker, Time-variant channel estimation using discrete prolate spheroidal sequences, *IEEE Trans. Signal Process*., 53(9): 3597–3607, September 2005.

[31] Technical Specification Group Radio Access Network, Radio Link Control (RLC) Protocol Specification, 3rd Generation Partnership Project (3GPP), Tech. Rep. TS 25.322 Version 8.4.0, March 2009.

[32] Technical Specification Group Radio Access Network, Multiplexing and Channel Coding (FDD), 3rd Generation Partnership Project (3GPP), Tech. Rep. TS 25.212 Version 8.5.0, March 2009.

[33] Technical Specification Group Radio Access Network, Medium Access Control (MAC) Protocol Specification, 3rd Generation Partnership Project (3GPP), Tech. Rep. TS 25.321 Version 7.0.0, March 2006.

[34] Technical Specification Group Radio Access Network, UTRA High Speed Downlink Packet Access (HSDPA); Overall Description; Stage 2, 3rd Generation Partnership Project (3GPP), Tech. Rep. TS 25.308 Version 5.0.0, September 2001.

[35] S.M. Kay, *Fundamentals of Statistical Signal Processing. Estimation Theory*, vol. 1, Prentice-Hall, 1993.

[36] D.J. Cichon and T. Kürner, *COST 231—Digital Mobile Radio towards Future Generation Systems*. COST, 1998, ch. 4.

[37] Technical Specification Group Radio Access Network, Spatial Channel Model for Multiple Input Multiple Output (MIMO) Simulations, 3rd Generation Partnership Project (3GPP), Tech. Rep. TS 25.996 Version 7.0.0, June 2007.